Polarizability and physical bounds on antennas in cylindrical and rectangular geometries

Gustafsson, Mats

2010

CODEN:LUTEDX/(TEAT-7195)/1-11/(2010)

Polarizability and physical bounds on antennas in cylindrical and rectangular geometries

Mats Gustafsson

Electromagnetic Theory
Department of Electrical and Information Technology
Lund University
Sweden

Mats Gustafsson
Mats.Gustafsson@eit.lth.se

Department of Electrical and Information Technology
Electromagnetic Theory
Lund University
P.O. Box 118
SE-221 00 Lund
Sweden

Editor: Gerhard Kristensson

Abstract

Recently developed physical bounds on antennas relate the directivity bandwidth product to the polarizability of the antenna structure. Although, the polarizability can be determined numerically for arbitrary objects, it is advantageous to have simple closed form expressions for canonical geometries. Here, rational approximations are presented for the polarizability of cylinders and planar rectangles.

1 Introduction

Physical bounds on antennas as introduced by Wheeler [14] and Chu [1] are mainly used to analyze bandwidth constraints on small antennas, where small often is quantified in terms of the radius, a, of the smallest circumscribing sphere. It is common to define antennas as small if $k_0 a \leq 1$ and sometimes $k_0 a \leq 1/2$, where k_0 denotes the resonance wavenumber. The antenna identity and its associated physical bounds introduced in [2–4, 10] are valid for lossless antennas of arbitrary shape as well as size. They express the antenna performance in terms of the polarizability of the antenna structure or of an arbitrary circumscribing geometry that provide a priori estimates and physical bounds, respectively. The results are identical to the bound by Thal [12] for the special case of circumscribing spheres. The bounds have also been verified against several antennas with electrical size up to $k_0 a \approx 1.5$.

Simple closed form expressions of the polarizability dyadics are known for geometries such as spheroids and elliptic disks [8, 11]. Numerical solutions can be used to compute them for arbitrary geometries. In this paper, we review the results for circumscribing spheroids and elliptic disks and determine simple approximations based on rational expressions for circumscribing cylinders and planar rectangles[1]. The results offer simple expressions for the physical bounds on D/Q for antennas circumscribed by these geometries.

2 Polarizability and physical bounds on D/Q

The physical bounds in [2–4, 10] are based on the antenna identity

$$\int_0^\infty \frac{(1-|\Gamma(k)|^2)D(k;\hat{\boldsymbol{r}},\hat{\boldsymbol{e}})}{k^4}\,\mathrm{d}k = \frac{\eta}{2}\big(\hat{\boldsymbol{e}}\cdot\boldsymbol{\gamma}_\mathrm{e}\cdot\hat{\boldsymbol{e}} + (\hat{\boldsymbol{r}}\times\hat{\boldsymbol{e}})\cdot\boldsymbol{\gamma}_\mathrm{m}\cdot(\hat{\boldsymbol{r}}\times\hat{\boldsymbol{e}})\big), \qquad (2.1)$$

where Γ denotes the reflection coefficient, D is the partial directivity, k the wavenumber, $\hat{\boldsymbol{r}}$ observation direction, and $\hat{\boldsymbol{e}}$ the (linear) polarization. The right-hand side contains the electric, $\boldsymbol{\gamma}_\mathrm{e}$, and magnetic, $\boldsymbol{\gamma}_\mathrm{m}$, polarizability dyadics[2] and the generalized (all spectrum) absorption efficiency

$$\eta = \int_0^\infty \frac{\sigma_\mathrm{a}(k;-\hat{\boldsymbol{r}},\hat{\boldsymbol{e}})}{k^2}\,\mathrm{d}k \Big/ \int_0^\infty \frac{\sigma_\mathrm{ext}(k;-\hat{\boldsymbol{r}},\hat{\boldsymbol{e}})}{k^2}\,\mathrm{d}k. \qquad (2.2)$$

[1] http://www.mathworks.com/matlabcentral/fileexchange/26806-antennaq

[2] Note that the polarizability dyadics, here denote by $\boldsymbol{\gamma}$, see [6], are also often denoted by $\boldsymbol{\alpha}$ [13] and $\mathbf{P}$ [8].

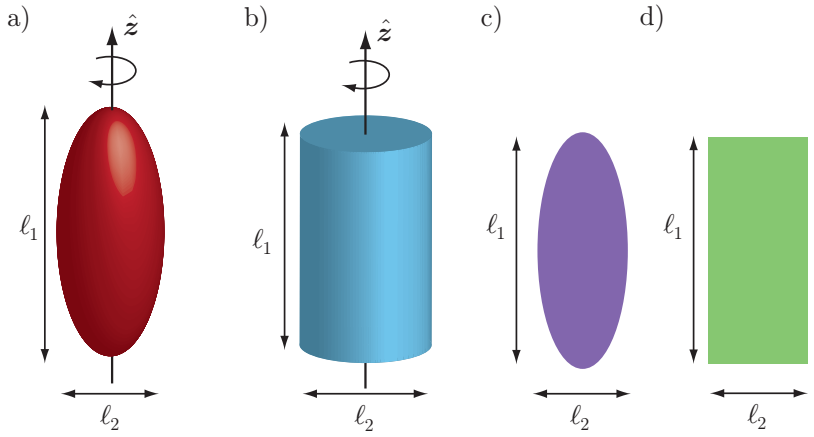

Figure 1: Illustrations of a) spheroids, b) cylinders, c) elliptic disks, and d) planar rectangles.

Here, σ_{ext} and σ_{a} are the extinction and absorption cross sections [6, 8], respectively. It is observed that $0 \leq \eta < 1$ and that $\eta \approx 1/2$ for many resonant antennas [4]. It is also shown that $\eta \leq 1/2$ for dipole antennas as $k_0 a \to 0$.

The identity (2.1) is used to derive the bound

$$\frac{D}{Q} \leq \frac{\eta k_0^3}{2\pi}\big(\hat{\boldsymbol{e}} \cdot \boldsymbol{\gamma}_{\text{e}} \cdot \hat{\boldsymbol{e}} + (\hat{\boldsymbol{r}} \times \hat{\boldsymbol{e}}) \cdot \boldsymbol{\gamma}_{\text{m}} \cdot (\hat{\boldsymbol{r}} \times \hat{\boldsymbol{e}})\big) \tag{2.3}$$

for linearly polarized antennas with a dominant simple resonance having $Q \gg 1$ [5]. The result (2.3) is valid for arbitrary antennas composed by electric and magnetic materials. It can be used to estimate the performance of many small antennas [4]. To bound the performance of any antenna circumscribed by an arbitrary geometry, the high-contrast polarizability dyadic $\boldsymbol{\gamma}_\infty$ is introduced. Variational principles [7, 9] show that

$$\boldsymbol{\gamma}_{\text{e}} \leq \boldsymbol{\gamma}_\infty \quad \text{and} \quad \boldsymbol{\gamma}_{\text{m}} \leq \boldsymbol{\gamma}_\infty \tag{2.4}$$

for any circumscribing geometry. Most antennas are constructed by non-magnetic materials. This simplifies (2.3) to

$$\frac{D}{Q} \leq \frac{\eta k_0^3}{2\pi}\hat{\boldsymbol{e}} \cdot \boldsymbol{\gamma}_\infty \cdot \hat{\boldsymbol{e}} = \frac{\eta k_0^3 \gamma}{2\pi}, \tag{2.5}$$

where $\gamma = \hat{\boldsymbol{e}} \cdot \boldsymbol{\gamma}_\infty \cdot \hat{\boldsymbol{e}}$ is the polarizability of the circumscribing geometry for the polarization $\hat{\boldsymbol{e}}$.

The polarizability dyadics are known for geometries such as spheroids and elliptic disks [8, 11]. For other geometries, they can be computed numerically. The high-contrast polarizability dyadic for the surface ∂V is determined from [8]

$$\boldsymbol{\gamma}_\infty \cdot \hat{\boldsymbol{e}} = \int_{\partial V} \boldsymbol{r}\, \varrho(\boldsymbol{r})\, \mathrm{dS}, \tag{2.6}$$

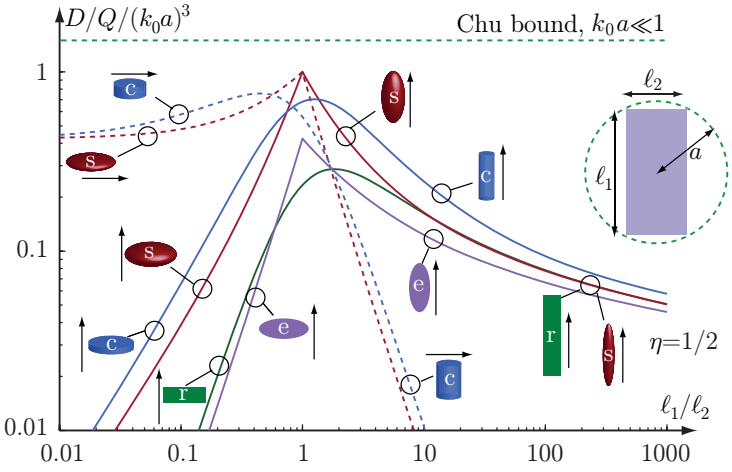

Figure 2: Physical bounds on D/Q for non-magnetic linearly polarized antennas circumscribed by spheroids (s), elliptic disks (e), cylinders (c), and planar rectangles (r).

where ϱ is the normalized surface charge density induced by an unit external electric field in the $\hat{\boldsymbol{e}}$-direction, see Fig. 3. The surface charge density can be computed from the integral equation [8]

$$\int_{\partial V} \frac{\varrho(\boldsymbol{r}')}{4\pi|\boldsymbol{r}-\boldsymbol{r}'|}\,\mathrm{dS}' = \hat{\boldsymbol{e}}\cdot\boldsymbol{r} + C, \tag{2.7}$$

where the constant C is determined such that the total charge on the object is zero, *i.e.*, $\int_{\partial V}\varrho\,\mathrm{dS} = 0$.

3 Circumscribing spheroids

Spheroids are body of revolution objects parameterized by

$$\left(\frac{2z}{\ell_1}\right)^2 + \left(\frac{2\rho}{\ell_2}\right)^2 \leq 1, \tag{3.1}$$

where $\rho = \sqrt{x^2+y^2}$, see Fig. 1. Introduce the semi-axis ratio $\xi = \ell_1/\ell_2$ and the radius $a = \max\{\ell_1,\ell_2\}/2$ of the smallest circumscribing sphere. There are simple closed form expression for the polarizability dyadics of spheroids [8, 11]. The rotational symmetry imply that they have the form

$$\boldsymbol{\gamma}_{\mathrm{s}} = \gamma_{\mathrm{sh}}(\hat{\boldsymbol{x}}\hat{\boldsymbol{x}} + \hat{\boldsymbol{y}}\hat{\boldsymbol{y}}) + \gamma_{\mathrm{sv}}\hat{\boldsymbol{z}}\hat{\boldsymbol{z}}, \tag{3.2}$$

where γ_{sh} and γ_{sv} denote the vertical and horizontal polarizability, respectively.

With a polarization along the axis of rotation, *i.e.*, vertical polarization, the polarizability, $\gamma_{\mathrm{sv}} = \hat{\boldsymbol{z}}\cdot\boldsymbol{\gamma}_{\mathrm{s}}\cdot\hat{\boldsymbol{z}}$, is

$$\frac{\gamma_{\mathrm{sv}}(\xi)}{a^3} = \frac{4\pi\xi}{3}\,\frac{e^3}{e-\xi\arccos(\xi)} \tag{3.3}$$

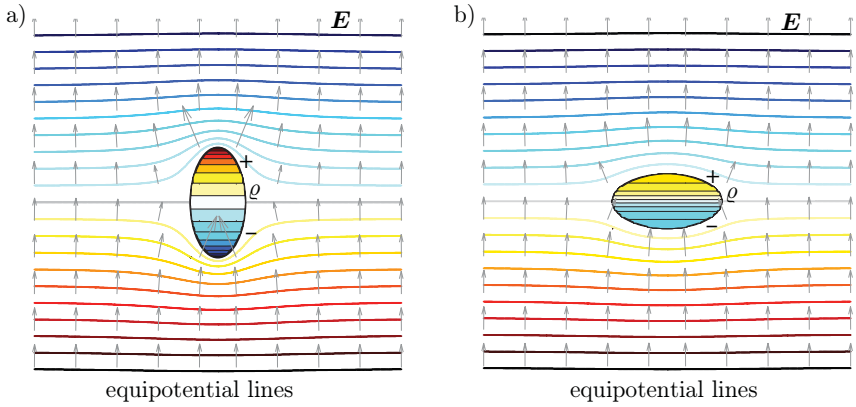

Figure 3: Equipotential lines and induced surface charge density on high-contrast spheroids with an incident electric field in the $\hat{\boldsymbol{z}}$-direction, see Fig. 1. a) semi-axis ratio $\xi = \ell_1/\ell_2 = 2$ (prolate case). b) semi-axis ratio $\ell_1/\ell_2 = 1/2$ (oblate case).

for the oblate case $\xi \leq 1$, where $e = \sqrt{1-\xi^2}$. The corresponding prolate case $\xi \geq 1$ is

$$\frac{\gamma_{\mathrm{sv}}(\xi)}{a^3} = \frac{4\pi}{3}\frac{e^3}{\ln(1+e) + \ln\xi - e}, \tag{3.4}$$

where $e = \sqrt{1-\xi^{-2}}$. This gives the asymptotic expansions

$$\frac{\gamma_{\mathrm{sv}}(\xi)}{a^3} \sim \begin{cases} \frac{4\pi\xi}{3} & \text{as } \xi \to 0 \\ \frac{4\pi}{3\left(\ln(2\xi)-1\right)} & \text{as } \xi \to \infty. \end{cases} \tag{3.5}$$

Note that γ_{sv}/a^3 vanishes linearly in the $\xi \to 0$ limit and logarithmically in the $\xi \to \infty$ limit. This behavior is similar for the rectangular and cylindrical cases analyzed in Secs 5 and 6, respectively. The logarithmic decay affects the accuracy in the approximation with rational functions.

The corresponding case with a polarization perpendicular to the axis of rotation, *i.e.*, horizontal polarization gives

$$\frac{\gamma_{\mathrm{sh}}(\xi)}{a^3} = \frac{8\pi}{3}\frac{e^3}{\arccos(\xi) - e\xi} \tag{3.6}$$

for the oblate case $\xi \leq 1$, where $e = \sqrt{1-\xi^2}$. The prolate case $\xi \geq 1$ is

$$\frac{\gamma_{\mathrm{sh}}(\xi)}{a^3} = \frac{8\pi}{3\xi^2}\frac{2e^3}{2e - \xi^{-2}\ln\frac{1+e}{1-e}}, \tag{3.7}$$

where $e = \sqrt{1-\xi^{-2}}$. With the asymptotic expansions

$$\frac{\gamma_{\mathrm{sh}}(\xi)}{a^3} \sim \begin{cases} \frac{16}{3} & \text{as } \xi \to 0 \\ \frac{8\pi}{3\xi^2} & \text{as } \xi \to \infty \end{cases} \tag{3.8}$$

The special case with a sphere, $\gamma_{\rm sv}(1) = \gamma_{\rm sh}(1) = 4\pi a^3$ gives $D/Q \le 2\eta k_0^3 a^3$. This reduces to the result $Q \ge 3/(2k_0^3 a^3)$ in [12] for small dipole antennas, $D = 3/2$, with $\eta = 1/2$.

4 Circumscribing elliptic disks

The elliptic disk is a planar geometry with simple closed form expressions for the polarizability [8]. The elliptic disks are defined by

$$\left(\frac{2z}{\ell_1}\right)^2 + \left(\frac{2x}{\ell_2}\right)^2 \le 1, \tag{4.1}$$

and $y = 0$. The polarizability dyadic has the form

$$\boldsymbol{\gamma}_{\rm e} = \gamma_{\rm eh}\hat{\boldsymbol{x}}\hat{\boldsymbol{x}} + \gamma_{\rm ev}\hat{\boldsymbol{z}}\hat{\boldsymbol{z}}, \tag{4.2}$$

where $\gamma_{\rm eh}(\xi) = \gamma_{\rm ev}(1/\xi)$. The polarizability is

$$\frac{\gamma_{\rm ev}}{a^3} = \frac{4\pi}{3}\frac{e^2}{\xi^{-2}\mathrm{E}(e^2) - \mathrm{K}(e^2)} \tag{4.3}$$

where $e = \sqrt{1-\xi^2}$ for $\xi < 1$ and for $\xi > 1$ it is

$$\frac{\gamma_{\rm ev}}{a^3} = \frac{4\pi}{3}\frac{e^2}{\mathrm{K}(e^2) - \mathrm{E}(e^2)} \tag{4.4}$$

where $e = \sqrt{1-\xi^{-2}}$ and K and E denote the complete elliptic functions of the first and second kinds, respectively. The asymptotic expansions are

$$\frac{\gamma_{\rm ev}}{a^3} \sim \begin{cases} \frac{4\pi\xi^2}{3} & \text{as } \xi \to 0 \\ \frac{4\pi}{3\left(\ln(4\xi)-1\right)} & \text{as } \xi \to \infty. \end{cases} \tag{4.5}$$

5 Circumscribing planar rectangles

Consider a rectangle in the xz-plane defined by $|z| \le \ell_1/2$, $|x| \le \ell_2/2$, and $y = 0$, see Fig. 1c. It has the circumscribing radius $a = \sqrt{\ell_1^2 + \ell_2^2}/2$ and the semi-axis ratio $\xi = \ell_1/\ell_2$. The polarizability dyadic has the form

$$\boldsymbol{\gamma}_{\rm r} = \gamma_{\rm rh}\hat{\boldsymbol{x}}\hat{\boldsymbol{x}} + \gamma_{\rm rv}\hat{\boldsymbol{z}}\hat{\boldsymbol{z}}, \tag{5.1}$$

where $\gamma_{\rm rh}(\xi) = \gamma_{\rm rv}(1/\xi)$. The polarizability dyadics are determined from the solution of the integral equation (2.7) that simplifies to

$$z = \int_{-\ell_1/2}^{\ell_1/2}\int_{-\ell_2/2}^{\ell_2/2} \frac{\varrho(x',z')}{4\pi\sqrt{(x-x')^2 + (z-z')^2}}\,\mathrm{d}x'\,\mathrm{d}z' \tag{5.2}$$

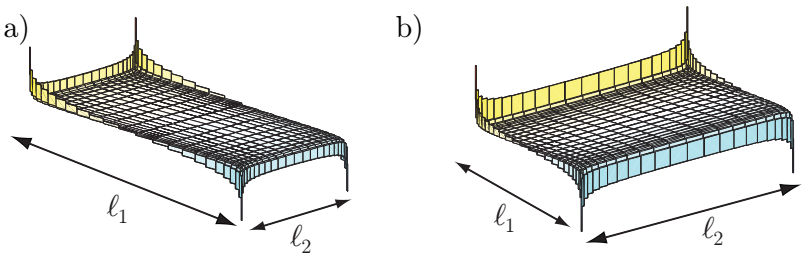

Figure 4: Charge distributions on planar rectangles with polarization aligned with the ℓ_1 side. a) $\xi = \ell_1/\ell_2 = 2$. b) $\xi = \ell_1/\ell_2 = 1/2$.

and (2.6) becomes

$$\gamma_{\rm rv} = \int_{-\ell_1/2}^{\ell_1/2} \int_{-\ell_2/2}^{\ell_2/2} z\varrho(x,z)\,{\rm d}x\,{\rm d}z. \tag{5.3}$$

The integral equation is solved with a method of moments approach using point matching and piecewise constant basis functions on rectangular elements. The symmetries $\varrho(x,z) = -\varrho(x,-z)$ and $\varrho(x,z) = \varrho(-x,z)$ are also used to reduce the number of unknowns. The normalized surface charge densities are depicted in Fig. 4 for the cases $\xi = 2$ and $\xi = 1/2$. Note that the charge densities are singular at the edges and corners.

The polarizability $\gamma_{\rm rv}$ is determined for $10^{-3} \le \xi \le 10^3$, see Fig. 2 for partial results. It is observed that the behaviors of $\gamma_{\rm rv}/a^3$ are different in the limits $\xi \to 0$ and $\xi \to \infty$. For $\xi \le 1$, $\gamma_{\rm rv}/(a^3\xi^2)$ has a simple shape, see Fig. 5a, that can be approximated accurately with simple rational functions, see Appendix A. Use of rational functions with numerator of second degree and denominator of third degree give the approximation

$$\frac{\gamma_{\rm rv}(\xi)}{a^3} \approx \xi^2 \frac{6.275 + 7.328\xi - 1.651\xi^2}{1 + 0.8\xi + 1.025\xi^2 + 1.242\xi^3}. \tag{5.4}$$

The interpolation error is shown in Fig. 5c. Note that the numerical data also has errors and that this error is of the order 10^{-2} to 10^{-3}.

The $\xi > 1$ case has a logarithmic decay similar to the spheroid (3.4) that is not suitable for fitting with rational functions. Instead, consider the quotient $\gamma_{\rm rv}/\gamma_{\rm sv}$ to reduce the effect of the logarithmic term. The infinite interval $\xi > 1$ is secondly transformed to the finite interval $0 < 1/\xi < 1$ to simplify the least-squares solution, see Fig. 5b. Fitting with rational functions give

$$\frac{\gamma_{\rm rv}(\xi)}{\gamma_{\rm sv}(\xi)} \approx \frac{1.001 + 18.098\xi^{-1} - 11.42\xi^{-2} + 2.266\xi^{-3}}{1 + 17.074\xi^{-1} - 0.309\xi^{-2} + 24.78\xi^{-3}} \tag{5.5}$$

with the relative error depicted in Fig. 5d.

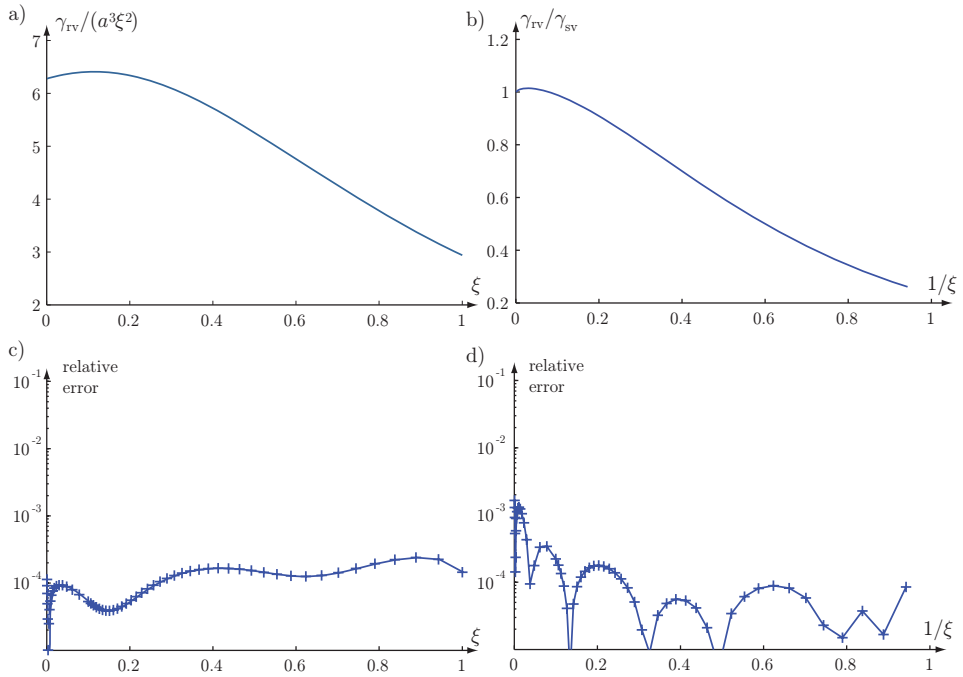

Figure 5: Normalized polarizability for planar rectangles. a) $\gamma_{\rm rv}/(a^3\xi^2)$ for $\xi > 1$. b) $\gamma_{\rm rv}/\gamma_{\rm sv}$ for $\xi \geq 1$. c,d) relative errors for the a,b cases.

6 Circumscribing cylinders

Consider a cylinder with height ℓ_1 and diameter ℓ_2, see Fig. 1b. The high-contrast polarizability dyadic has the form

$$\boldsymbol{\gamma}_{\rm c} = \gamma_{\rm ch}(\hat{\boldsymbol{x}}\hat{\boldsymbol{x}} + \hat{\boldsymbol{y}}\hat{\boldsymbol{y}}) + \gamma_{\rm cv}\hat{\boldsymbol{z}}\hat{\boldsymbol{z}}, \tag{6.1}$$

where $\gamma_{\rm ch}$ and $\gamma_{\rm cv}$ are the polarizabilities for the horizontal and the vertical polarizations, respectively. The induced surface charge density and the polarizability are determined for $10^{-3} \leq \xi \leq 10^3$ from (2.7) and (2.6) with the additional simplification due to the rotational symmetry, see Fig. 2 for partial results.

It is observed that the polarizability for the vertical polarization, $\gamma_{\rm cv}$, has similar polarizability as the corresponding spheroid. The effect of the logarithmic decay (3.5) is reduced by division with $\gamma_{\rm sv}$. The quantities $\gamma_{\rm cv}/(a^3\xi)$ and $\gamma_{\rm cv}/\gamma_{\rm sv}$ are fitted to rational functions. For $\xi \leq 1$, it gives the rational approximation

$$\frac{\gamma_{\rm cv}(\xi)}{a^3} \approx \xi \frac{6.241 + 59.056\xi + 36.097\xi^2}{1 + 5.2995\xi - 1.92\xi^2 + 7.453\xi^3} \tag{6.2}$$

and for $\xi > 1$ it gives

$$\frac{\gamma_{\rm cv}(\xi)}{\gamma_{\rm sv}(\xi)} \approx \frac{1.135 + 24.004\xi^{-1} - 4.355\xi^{-2}}{1 + 13.851\xi^{-1} - 6.093\xi^{-2} + 21.706\xi^{-3}}. \tag{6.3}$$

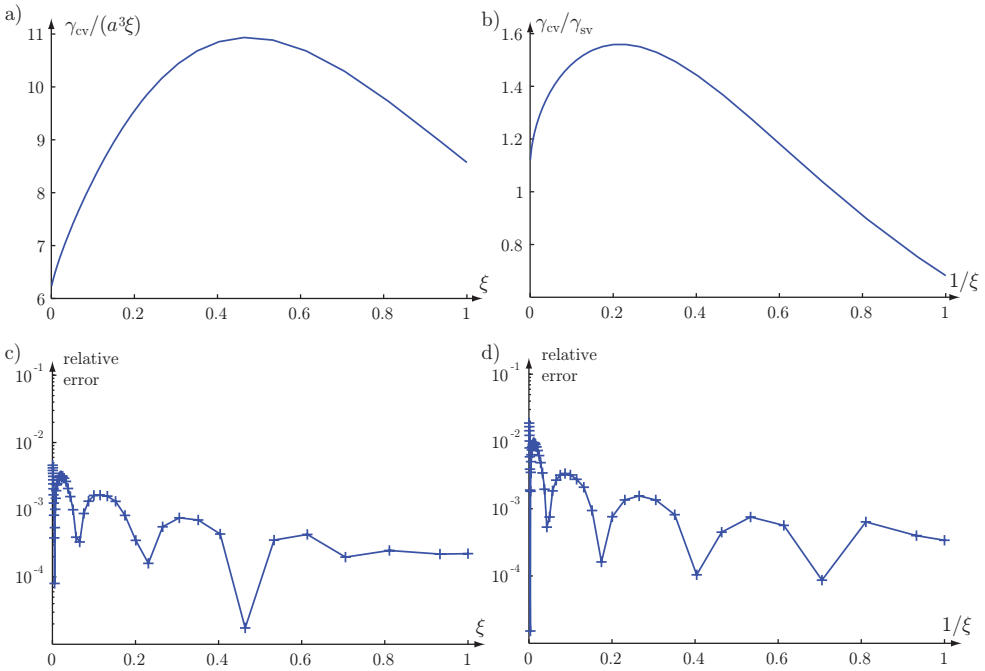

Figure 6: Normalized polarizability for cylinders with polarization along the cylinder axis. a) $\gamma_{cv}/(\xi a^3)$ for $\xi \leq 1$. b) γ_{cv}/γ_{sv} for $\xi > 1$. c,d) relative errors for the a,b cases.

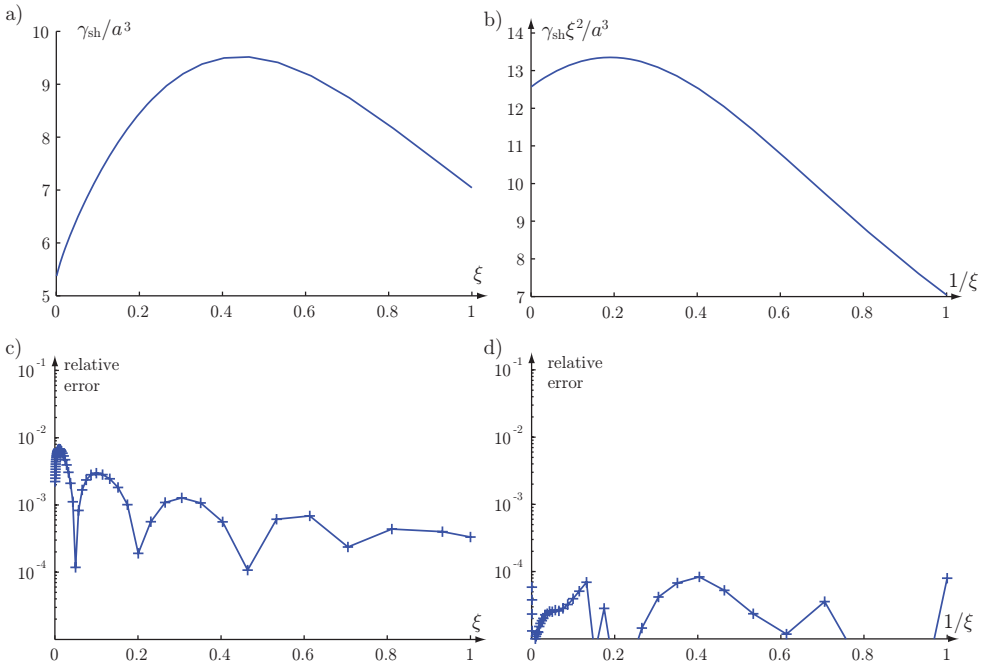

Figure 7: Normalized polarizability for cylinders with polarization perpendicular to the cylinder axis. a) γ_{ch}/a^3 for $\xi \leq 1$. b) $\gamma_{ch}\xi^2/a^3$ for $\xi > 1$. c,d) relative errors for the a,b cases.

The polarizability for the horizontal polarization $\gamma_{\rm ch}$ is also similar to the corresponding case for the spheroid (3.6) and (3.7). For $\xi \leq 1$ the analytically known value $\gamma_{\rm ch}(0) = a^3 16/3$ is used to give the rational approximation

$$\frac{\gamma_{\rm ch}(\xi)}{a^3} \approx \frac{16/3 + 59.47\xi + 28.064\xi^2}{1 + 6.087\xi - 2.935\xi^2 + 9.032\xi^3} \tag{6.4}$$

and for $\xi > 1$ the fitting gives

$$\frac{\gamma_{\rm ch}(\xi)}{a^3} \approx \xi^{-2} \frac{12.565 + 13.932\xi^{-1} - 2.804\xi^{-2}}{1 + 0.456\xi^{-1} + 1.1\xi^{-2} + 0.809\xi^{-3}}. \tag{6.5}$$

The interpolation functions and the relative errors are depicted in Fig. 7.

7 Conclusions

Simple rational expressions are provided for the polarizability of planar rectangles and cylinders. The rational approximations are determined from method of moment solutions of the charge density. The results are used to give simple closed form expressions for the physical bounds on D/Q for antennas circumscribed by cylinders and rectangles.

8 Acknowledgment

This work has been partially supported by The Swedish Governmental Agency for Innovation Systems (VINNOVA) within the IMT-advanced and beyond project.

Appendix A Least squares fitting of rational functions

The least squares solution can be used to fit rational functions to data. Consider the following approximation with rational functions

$$f(x) \approx \frac{\sum_{m=0}^{N_1} p_m x^m}{1 + \sum_{n=1}^{N_2} q_n x^n}, \tag{A.1}$$

where the function $f(x)$ is given for $x_1 \leq x \leq x_2$ and N_1, $N_2 \geq 0$ integers.

Multiply with the denominator to rewrite into a form suitable for least-squares solution, *i.e.*,

$$\min_{p_m, q_n} \int \left| f(x) - \sum_{m=0}^{N_1} p_m x^m + \sum_{n=1}^{N_2} q_n x^n f(x) \right|^2 \, {\rm d}x. \tag{A.2}$$

This is an over determined linear system that can be solved in the least squares approximation. The problem is that the solution depends on the chosen orders N_2

and N_3 as well as the used sample points and their values, *e.g.*, a linear scaling $x \to 2x$ usually changes the results. It is also common that interpolations of f and $1/f$ give different results. These problems are reduced if $f(x)$ is approximately constant over the interpolation interval, see Figs 5, 6, and 7.

References

[1] L. J. Chu. Physical limitations of omni-directional antennas. *Appl. Phys.*, **19**, 1163–1175, 1948.

[2] A. Derneryd, M. Gustafsson, G. Kristensson, and C. Sohl. Application of gain-bandwidth bounds on loaded dipoles. *IET Microwaves, Antennas & Propagation*, **3**(6), 959–966, 2009.

[3] M. Gustafsson, C. Sohl, and G. Kristensson. Physical limitations on antennas of arbitrary shape. *Proc. R. Soc. A*, **463**, 2589–2607, 2007.

[4] M. Gustafsson, C. Sohl, and G. Kristensson. Illustrations of new physical bounds on linearly polarized antennas. *IEEE Trans. Antennas Propagat.*, **57**(5), 1319–1327, May 2009.

[5] M. Gustafsson and S. Nordebo. Bandwidth, Q factor, and resonance models of antennas. *Progress in Electromagnetics Research*, **62**, 1–20, 2006.

[6] J. D. Jackson. *Classical Electrodynamics*. John Wiley & Sons, New York, second edition, 1975.

[7] D. S. Jones. Scattering by inhomogeneous dielectric particles. *Quart. J. Mech. Appl. Math.*, **38**, 135–155, 1985.

[8] R. E. Kleinman and T. B. A. Senior. Rayleigh scattering. In V. V. Varadan and V. K. Varadan, editors, *Low and high frequency asymptotics*, volume 2 of *Handbook on Acoustic, Electromagnetic and Elastic Wave Scattering*, chapter 1, pages 1–70. Elsevier Science Publishers, Amsterdam, 1986.

[9] D. Sjöberg. Variational principles for the static electric and magnetic polarizabilities of anisotropic media with perfect electric conductor inclusions. *J. Phys. A: Math. Theor.*, **42**, 335403, 2009.

[10] C. Sohl and M. Gustafsson. A priori estimates on the partial realized gain of Ultra-Wideband (UWB) antennas. *Quart. J. Mech. Appl. Math.*, **61**(3), 415–430, 2008.

[11] A. F. Stevenson. Solution of electromagnetic scattering problems as power series in the ratio (dimension of scatterer)/wavelength. *J. Appl. Phys.*, **24**(9), 1134–1142, September 1953.

[12] H. L. Thal. New radiation Q limits for spherical wire antennas. *IEEE Trans. Antennas Propagat.*, **54**(10), 2757–2763, October 2006.

[13] J. van Bladel. *Electromagnetic Fields*. IEEE Press, Piscataway, NJ, second edition, 2007.

[14] H. A. Wheeler. Fundamental limitations of small antennas. *Proc. IRE*, **35**(12), 1479–1484, 1947.